Shape transitions in ^{148}Sm

Alan L. Goodman
Physics Department, Tulane University, New Orleans, Louisiana 70118
(Received 21 May 1993)

The finite-temperature Hartree-Fock-Bogoliubov cranking equation is solved for ^{148}Sm. The phase diagram contains three shape transition lines. For certain rotational frequencies, there is oblate noncollective rotation at low temperatures, prolate and triaxial collective rotation at intermediate temperatures, and oblate noncollective rotation at higher temperatures. A new oblate region at low T and ω is caused by the pairing interaction.

PACS number(s): 21.60.Jz, 27.60.+j

I. INTRODUCTION

The shape of a nucleus is strongly dependent on its temperature. Increasing the temperature causes shape transitions. In mean-field theories shape transitions occur suddenly at critical temperatures. However, when statistical fluctuations in the shape are included, these shape transitions then occur gradually, or they may be obscured. Extensive experiments on the giant dipole resonance provide evidence for thermal shape transitions and fluctuations [1,2].

Shape transitions in hot rotating nuclei have been described by two mean-field theories: the microscopic finite-temperature Hartree-Fock-Bogoliubov cranking (FTHFBC) theory [3] and the macroscopic Landau theory of phase transitions [4,5]. Previous investigations using these two theories predict phase diagrams which contain only one shape transition line in the temperature versus rotational frequency plane. This transition line is defined by the frequency-dependent critical temperature $T_c(\omega)$. For temperatures below T_c the shape is prolate or triaxial and the rotation is collective. For temperatures above T_c the shape is oblate and the rotation is noncollective. The giant dipole resonance experiments furnish evidence for this shape transition.

The question addressed in this article is whether the phase diagram for a hot rotating nucleus can have more than one shape transition line. Previous FTHFB calculations for nonrotating ^{148}Sm nuclei suggest that this nucleus may have more than one shape transition line [6]. At spin zero ^{148}Sm has two shape transitions. The equilibrium shape is spherical for temperatures below $T_{c1}=0.40$ MeV. When the temperature rises above T_{c1}, the equilibrium shape suddenly becomes prolate. At a second critical temperature, $T_{c2}=0.91$ MeV, the equilibrium shape suddenly returns to spherical.

The first shape transition at T_{c1} is caused by a delicate balance between the pairing interaction (which favors spherical shapes) and the quadrupole interaction (which favors deformed shapes). For temperatures below T_{c1} the pairing interaction is more influential than the quadrupole interaction, so that the equilibrium shape is spherical. The critical temperature for the elimination of pairing correlations is normally less than the critical temperature for the elimination of deformation. When the temperature increases to T_{c1}, the pairing interaction becomes less influential than the quadrupole interaction, and the shape becomes deformed.

The second shape transition at T_{c2} is the conventional transition which occurs in other nuclei. The deformed shape for $T<T_{c2}$ is caused by shell effects. At T_{c2} the thermal particle-hole excitations eliminate this shell effect, and the shape becomes spherical.

This previous ^{148}Sm FTHFB calculation was restricted to spin zero. The purpose of this article is to extend this calculation to finite spins. Do the critical temperatures T_{c1} and T_{c2} at $\omega=0$ provide the end points of two distinct shape transition lines $T_{c1}(\omega)$ and $T_{c2}(\omega)$, or do T_{c1} and T_{c2} at $\omega=0$ give the two end points of one shape transition line $T_c(\omega)$? For either possibility, the phase diagram for ^{148}Sm is probably topologically different from the phase diagrams previously encountered for other hot rotating nuclei.

II. FINITE-TEMPERATURE HFB CRANKING CALCULATIONS

For each combination of temperature and spin, the equilibrium shape is determined by the self-consistent solution of the FTHFBC equation [7,8]

$$\begin{bmatrix} \mathcal{H} & \Delta \\ -\Delta^* & -\mathcal{H}^* \end{bmatrix} \begin{bmatrix} U_i \\ V_i \end{bmatrix} = E_i \begin{bmatrix} U_i \\ V_i \end{bmatrix} . \tag{1}$$

The Hartree-Fock Hamiltonian $\mathcal{H}$ includes the cranking term $-\omega J_x$, where ω is the angular velocity. The pair potential is Δ. The eigenvectors (U_{ij},V_{ij}) define the quasiparticle operators, and the eigenvalues E_i are the quasiparticle energies. The quasiparticle occupation probability is

$$f_i=\frac{1}{1+e^{E_i/T}} , \tag{2}$$

where T is the temperature. The mean fields $\mathcal{H}$ and Δ are calculated self-consistently with the pairing plus quadrupole interaction of Kumar and Baranger [9].

The quadrupole deformation parameters β and γ are shown in Figs. 1 and 2. The spin dependence of the

 ©1993 The American Physical Society

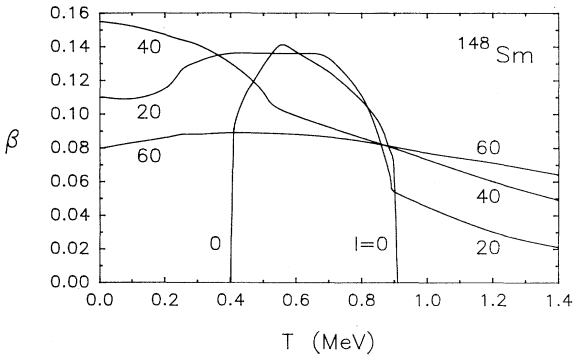

FIG. 1. The quadrupole deformation β versus the temperature T for ^{148}Sm. The spin is I.

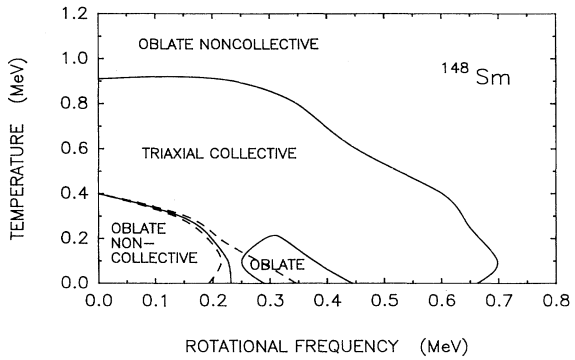

FIG. 3. Phase diagram for ^{148}Sm. The critical temperature T_c versus the rotational frequency ω.

shape transitions is more complex than that observed in previous calculations. For spin $I=0$ the shape is spherical for temperatures below $T_{c1}=0.40$ MeV and above $T_{c2}=0.91$ MeV. For temperatures between T_{c1} and T_{c2} the shape is prolate. These shape transitions were discussed in Sec. I and in Ref. [6]. For $I=10$ the shape is nearly prolate and the rotation is collective for temperatures up to $T_c=0.92$ MeV; at higher temperatures an oblate shape rotates noncollectively ($\gamma=-60°$). For $I=20$ there is oblate noncollective rotation for temperatures below $T_{c1}=0.18$ MeV and above $T_{c2}=0.90$ MeV; for temperatures between T_{c1} and T_{c2} the shape is triaxial. For $I=30$ there is oblate noncollective rotation at $T_{c1}=0$ and $T>T_{c2}=0.80$ MeV; for $T_{c1}<T<T_{c2}$ the shape is triaxial. For $I=40$ the shape is triaxial for $T<T_c=0.56$ MeV; for $T>T_c$ there is oblate noncollective rotation. For $I=50$ and 60 there is oblate noncollective rotation at all temperatures. Figures 1 and 2 demonstrate that for ^{148}Sm the temperature dependence of the shape is completely different at each spin. Different spins display different thermally induced shape transitions.

The phase diagram for the ^{148}Sm shape is given in Fig. 3. The shape transition line which begins at $(\omega,T)=(0,0.91$ MeV) separates a prolate and triaxial collective phase from an oblate noncollective phase. This is the conventional shape transition line predicted for other nuclei by the FTHFBC [3] and Landau [4,5] mean-field theories. The phase diagram contains two additional shape transition lines at low temperatures and low spins. These two new transition lines were not seen in previous FTHFBC or Landau calculations. They demarcate two new regions for the oblate noncollective phase.

One of the new oblate regions occurs at $T<0.25$ MeV and 0.25 MeV $<\omega<0.45$ MeV. This region is caused by crossings of prolate and oblate bands along the yrast line. This oblate phase is eliminated by a very small thermal excitation. This oblate region is bounded by a second-order phase transition line.

What causes the new shape transition line which begins at $(\omega,T)=(0,0.40$ MeV)? Why is there a new oblate region adjacent to this transition line? First consider the vertical axis of the phase diagram ($\omega=0$). There is a critical temperature $T_{c1}=0.40$ MeV. The shape is spherical for $T<T_{c1}$ because of the strong pair correlations, and the shape is prolate for $T>T_{c1}$. For a spherical shape, any rotation axis is a symmetry axis, so the rotation must be noncollective rather than collective. Then the oblate shape is energetically favored over the prolate shape. Consequently, if a rotation is applied to the spherical shape at $\omega=0$ and $T<0.40$ MeV, then the result is oblate noncollective rotation. It should be emphasized that this new region for the oblate phase exists because of the strong pairing correlations. If the temperature and rotational frequency are increased sufficiently, then the pair correlations weaken, and there is a shape transition from the oblate phase to the prolate and triaxial phase.

Is this phase transition first order or second order? Phases 1 and 2 have an nth-order phase transition at constant T and ω if

$$\left[\frac{\partial^n F_1'}{\partial T^n}\right]_\omega \neq \left[\frac{\partial^n F_2'}{\partial T^n}\right]_\omega , \tag{3}$$

and

$$\left[\frac{\partial^n F_1'}{\partial \omega^n}\right]_T \neq \left[\frac{\partial^n F_2'}{\partial \omega^n}\right]_T , \tag{4}$$

where F' is the free energy in the rotating frame

$$F'=E-TS-\omega J , \tag{5}$$

and the energy E, spin I, and entropy S are

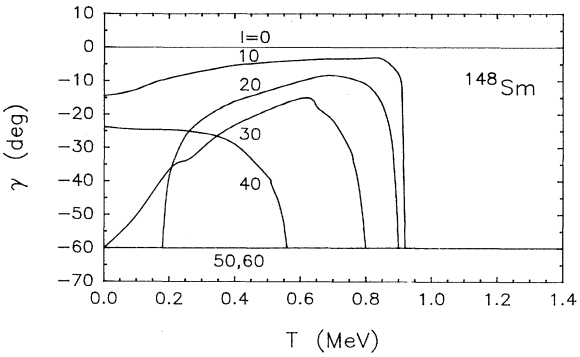

FIG. 2. The quadrupole deformation γ versus the temperature T for ^{148}Sm. The spin is I.

$$E=\langle H\rangle \ , \tag{6}$$

$$[I(I+1)]^{1/2}=J=\langle J_x\rangle \ , \tag{7}$$

$$S=-\sum_i [f_i \ln f_i+(1-f_i)\ln(1-f_i)] \ . \tag{8}$$

Substituting the thermodynamic relations

$$S=-\left[\frac{\partial F'}{\partial T}\right]_\omega \ , \tag{9}$$

$$J=-\left[\frac{\partial F'}{\partial \omega}\right]_T \ , \tag{10}$$

into Eqs. (3) and (4), it follows that a first-order transition at constant T and ω occurs if

$$F'_1=F'_2 \ , \tag{11}$$

$$S_1\neq S_2 \ , \tag{12}$$

$$J_1\neq J_2 \ . \tag{13}$$

A second-order transition occurs if

$$F'_1=F'_2 \ , \tag{14}$$

$$S_1=S_2 \ , \tag{15}$$

$$J_1=J_2 \ , \tag{16}$$

and the first derivatives of S and J with respect to T and ω are discontinuous at the transition.

These conditions are checked by graphing $F'(\omega)$ at constant T and $F'(T)$ at constant ω. For example, Fig. 4 is the isothermal function $F'(\omega)$ for $T=0.3$ MeV. It has the loop which characterizes a first-order phase transition. For spins $I<0.75$, there are stable states with oblate noncollective rotation. For $0.75<I<1.00$, there are metastable states with oblate noncollective rotation. For $1.00<I<1.25$, the states are unstable. For $1.25<I<2.00$, there are metastable states with prolate collective rotation. For $I>2.00$, there are stable states with prolate collective rotation. Stable states correspond to absolute minima in a free energy surface, whereas metastable states correspond to relative minima. At the crossing point in the loop there are two states, which by construction have the same values for T, ω, and F'. The two states correspond to degenerate minima in a free energy surface. The value of ω at the crossing point is the crossing or critical frequency $\omega_c=0.143$ MeV. Equation (10) states that the slope of $F'(\omega)$ gives the spin. Therefore, the two states at the crossing point have different spins, $I_1=0.75$ and $I_2=2.00$. So conditions (1) and (13) for a first-order phase transition are satisfied. Condition (12) is met by the loop in $F'(T)$ at constant ω. The conclusion is that this phase transition is first order.

This exercise was repeated for other temperatures below 0.4 MeV to determine how the critical frequency ω_c varies with T. The function $\omega_c(T)$ is the shape transition line in Fig. 3 which begins at $(\omega,T)=(0,0.4$ MeV). This transition line is first order, except for the point at $(\omega,T)=(0,0.4$ MeV), which marks a second-order transition. To the left of this solid line are stable oblate states, and to the right are stable prolate and triaxial states. The two dashed lines in Fig. 3 mark the limits of the metastable states. The metastable prolate and triaxial states lie between the inner dashed line and the solid line. The metastable oblate states are between the solid line and the outer dashed line. This metastable oblate region overlaps with the stable oblate region at $T<0.25$ MeV and 0.25 MeV $<\omega<0.45$ MeV. In this overlap region metastable and stable oblate states coexist at the same (ω,T). However, they are physically distinct states which have different spins, where I (stable) ≥ 18 and I(metastable) ≤ 12.

The phase diagram of Fig. 3 is expressed in the temperature-rotational frequency plane. This phase diagram can also be given in the temperature-angular momentum plane, as in Fig. 5. The primary difference is that the new oblate region at low T and ω is significantly smaller. This difference can be explained by considering the moment of inertia

$$\mathcal{J}=[I(I+1)]^{1/2}/\omega \ . \tag{17}$$

If ω is small and $T=0$ and the pairing plus quadrupole interaction is used, then the HFB moment of inertia is given by the Belyaev cranking formula [10]

$$\mathcal{J}=2\sum_{kk'>0}\frac{|\langle k|J_x|k'\rangle|^2}{E_k+E_{k'}}(u_k v_{k'}-u_{k'}v_k)^2 \ , \tag{18}$$

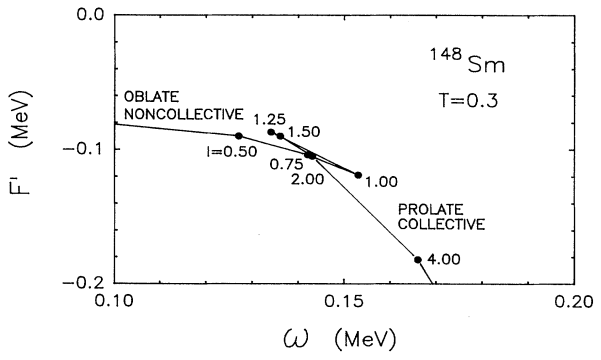

FIG. 4. The free energy in a rotating frame F' versus the rotational frequency ω. The temperature is 0.3 MeV. The crossing frequency is ω_c. The spin is I.

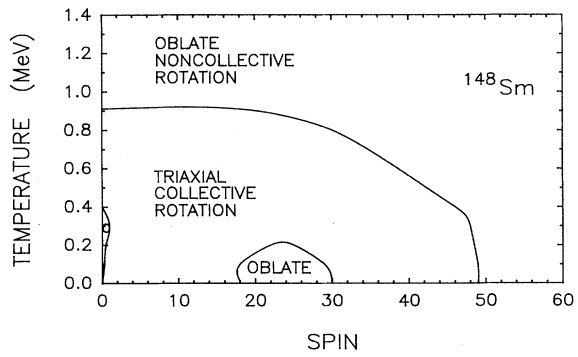

FIG. 5. Phase diagram for ^{148}Sm. The critical temperature T_c versus the spin I. The O denotes oblate.

where $|k\rangle$ are the Hartree-Fock single particle orbitals. For the oblate noncollective phase, the x axis is a symmetry axis, so that

$$J_x|k\rangle = m_k|k\rangle \ , \tag{19}$$

where m denotes m_x. Therefore, the matrix elements of J_x in Eq. (18) equal zero if $k \neq k'$. If $k=k'$, then the uv factor in Eq. (18) equals zero. Consequently, every term in the sum (18) vanishes. Therefore $\mathcal{I}=0$ for a small rotational frequency about a symmetry axis at zero temperature. Then Eq. (17) gives $I=0$ at $T=0$, even though $\omega \neq 0$. At finite temperature and small ω, $\mathcal{I}$ is small but not zero, so that a small spin occurs. This explains why the new oblate region at low T and ω is smaller in the (I,T) plane than in the (ω,T) plane.

The FTHFBC equation determines how the pair gap Δ varies with temperature and spin. For example, Fig. 6 shows how the proton and neutron pair gaps vary with spin for $T=0.1$ MeV. The proton gap vanishes at $I=40$, and the neutron gap vanishes at $I=16$. The shape transitions affect the pair gaps. For most nuclei the slope $d\Delta/dI$ is zero at $I=0$. However, Fig. 6 has $d\Delta/dI$ negative at small I because of the shape transition from oblate to triaxial at $I=0.3$. The proton gap increases at $I=18$ because of the transition from triaxial to oblate. Figure 7 shows how the proton gap depends on the temperature for $I=24$. The proton gap disappears at the critical temperature $T_c=0.69$ MeV.

III. STATISTICAL SHAPE FLUCTUATIONS

The FTHFBC equation determines the equilibrium shape for each combination of temperature and angular momentum. This is the shape which minimizes the free energy

$$F(\beta,\gamma;I,T)=E-TS \ . \tag{20}$$

Since a nucleus is a small system, there are significant statistical fluctuations of the shape around the equilibrium value. These fluctuations generate the shape probability distribution

$$P(\beta,\gamma;I,T) \propto \exp[-F(\beta,\gamma;I,T)/T] \ . \tag{21}$$

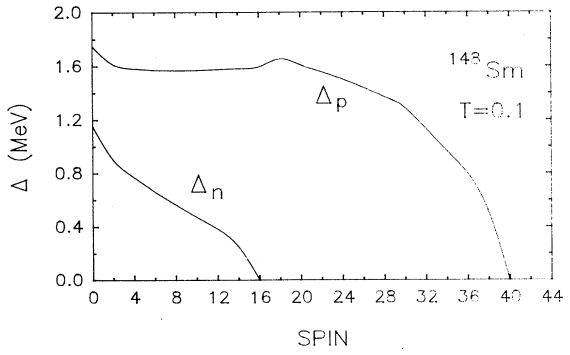

FIG. 6. The proton pair gap Δ_p and the neutron pair gap Δ_n versus the spin I for ^{148}Sm The temperature is 0.1 MeV.

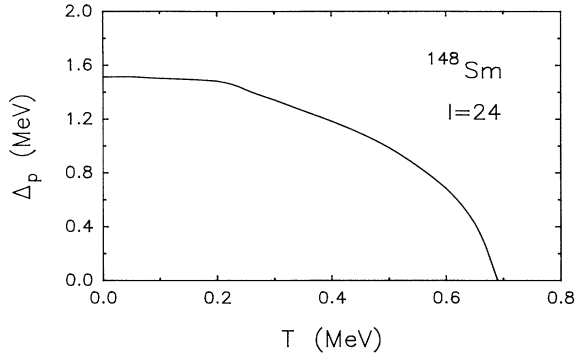

FIG. 7. The proton pair gap Δ_p versus the temperature T for ^{148}Sm. The spin is 24.

The shape fluctuations sometimes obscure the shape transitions predicted by mean-field theories.

This section considers the effect of shape fluctuations on electric quadrupole moments. The intrinsic quadrupole moments with respect to the rotation axis are [11]

$$Q_0' = \frac{3}{(5\pi)^{1/2}} ZeR^2\beta \sin(\gamma-30°) \ , \tag{22}$$

$$Q_2' = -\frac{3}{(10\pi)^{1/2}} ZeR^2\beta \cos(\gamma-30°) \ . \tag{23}$$

For an asymmetric rotor with large angular momentum, the static electric quadrupole moment is

$$Q \approx Q_0' \ , \tag{24}$$

and the $B(E2)$ value is [12]

$$B(E2, I \rightarrow I\pm 2) \approx \frac{5}{16\pi}(Q_2')^2 \ . \tag{25}$$

For oblate noncollective rotation $\gamma=-60°$ and the $B(E2)$ value is zero. Equations (24) and (25) are generally not valid at small spins. Nevertheless Q_0' and $(Q_2')^2$ remain useful as measures of the intrinsic shape even at low spins. For given temperature and spin, the FTHFBC equilibrium shape (β,γ) defines the HFB values of Q and

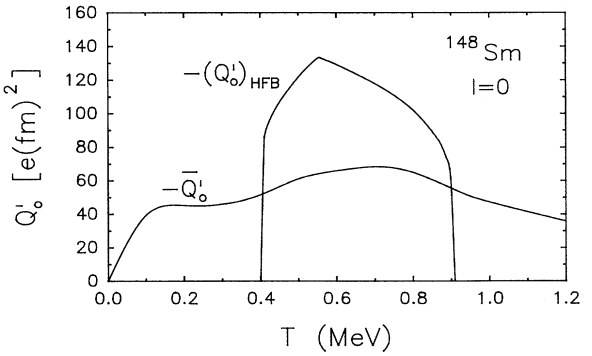

FIG. 8. The intrinsic quadrupole moment with respect to the rotation axis Q_0' versus the temperature T for ^{148}Sm. The spin is 0.

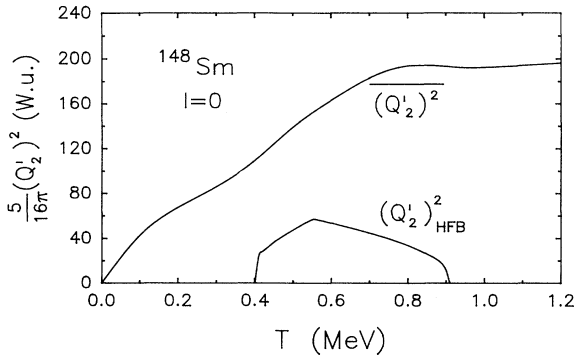

FIG. 9. The square of the intrinsic quadrupole moment with respect to the rotation axis Q'_2 versus the temperature T for ^{148}Sm. The spin is 0.

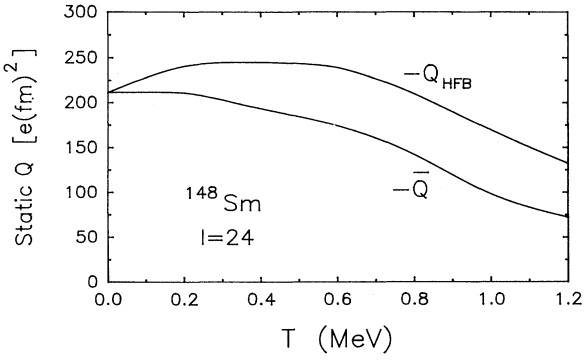

FIG. 11. The static electric quadrupole moment Q versus the temperature T for ^{148}Sm. The spin is 24.

$B(E2)$ via Eqs. (22)–(25). When the shape fluctuations are included, then the static electric quadrupole moment acquires the average value

$$\overline{Q}(I,T)=\langle Q\rangle=\frac{\int Q(\beta,\gamma)P(\beta,\gamma;I,T)d\tau}{\int P(\beta,\gamma;I,T)d\tau}\ , \tag{26}$$

where the metric

$$d\tau=\beta^4|\sin3\gamma|d\beta d\gamma\ .$$

There is a similar equation for the average $B(E2)$ value.

Figures 8 and 9 give Q'_0 and $(Q'_2)^2$ versus the temperature for spin zero. The FTHFB equilibrium shape is spherical ($\beta=0$) for temperatures below $T_{c1}=0.40$ MeV and above $T_{c2}=0.91$ MeV, and it is prolate ($\gamma=0°$) for the intermediate temperatures $T_{c1}<T<T_{c2}$. Consequently the HFB values for Q'_0 and $(Q'_2)^2$ are nonzero only for $T_{c1}<T<T_{c2}$. In contrast, when shape fluctuations are included, the averages $\langle Q'_0\rangle$ and $\langle (Q'_2)^2\rangle$ are nonzero for all positive temperatures. So the shape transitions at T_{c1} and T_{c2} predicted by the mean-field theory are obscured by the fluctuations. However, there are still residual signs of the transitions in the equilibrium shape at T_{c1} and T_{c2}: Observe that $\langle Q'_0\rangle$ has larger values in the temperature interval $T_{c1}<T<T_{c2}$ than at other temperatures. Similarly $\langle (Q'_2)^2\rangle$ increases more rapidly at T_{c1}.

Figure 10 gives the $B(E2)$ value versus the temperature for spin 24. The FTHFB equilibrium state is oblate noncollective rotation ($\gamma=-60°$) for temperatures below $T_{c1}=0.20$ MeV and above $T_{c2}=0.87$ MeV, and it is triaxial collective rotation for intermediate temperatures $T_{c1}<T<T_{c2}$. In contrast, when shape fluctuations are included, the average $B(E2)$ value is nonzero for all positive temperatures. This makes it more difficult to see the shape transitions at T_{c1} and T_{c2} predicted by the mean-field theory. Nevertheless, the average $B(E2)$ value has a more rapid increase in the interval $T_{c1}<T<T_{c2}$, which is a residual signal of the transitions in the equilibrium shape at T_{c1} and T_{c2}.

Figure 11 gives the static quadrupole moment Q versus the temperature for spin 24. The HFB value of Q does not provide direct evidence for the shape transitions at T_{c1} and T_{c2}. This is primarily because oblate noncollective rotation and prolate collective rotation both yield negative static quadrupole moments. When shape fluctuations are included, one obtains an average static moment which is not substantially different from the HFB static moment.

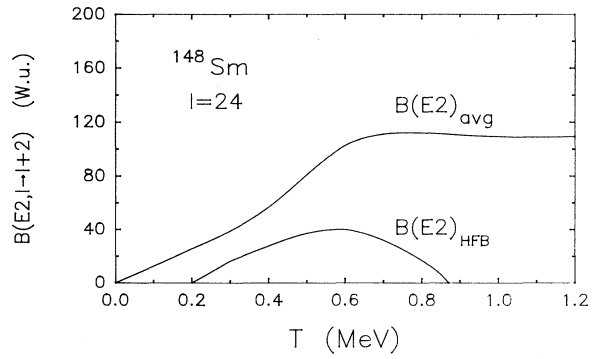

FIG. 10. The $B(E2)$ value versus the temperature T for ^{148}Sm. The spin is 24.

IV. CONCLUSIONS

Previous FTHFBC and Landau mean-field calculations predicted that hot rotating nuclei have phase diagrams which contain only one shape transition line in the temperature-spin plane. The question addressed in this article is whether some nuclei have more than one shape transition line. This FTHFBC calculation for ^{148}Sm gives a phase diagram with three shape transition lines. The oblate noncollective phase occurs in a new region at low temperatures and low rotational frequencies. This oblate phase occurs because the pairing interaction dominates over the quadrupole interaction at low T and ω. Raising T or ω weakens the effectiveness of the pairing interaction more than it weakens the quadrupole interaction. This causes a transition from the oblate noncollective phase to the prolate and triaxial collective phase.

The effect of statistical shape fluctuations on static quadrupole moments and $B(E2)$ values was calculated. These fluctuations smooth out the new shape transitions and make it difficult to detect their presence.

ACKNOWLEDGMENT

This work was supported in part by the National Science Foundation.

[1] J. Gaardhoje, Annu. Rev. Nucl. Part. Sci. **42**, 483 (1992).
[2] K. Snover, Annu. Rev. Nucl. Part. Sci. **36**, 545 (1986).
[3] A. L. Goodman, Phys. Rev. C **35**, 2338 (1987); **37**, 2162 (1988); **38**, 977 (1988); **38**, 1092 (1988); **39**, 2008 (1989).
[4] Y. Alhassid, S. Levit, and J. Zingman, Phys. Rev. Lett. **57**, 539 (1986).
[5] Y. Alhassid, J. Zingman, and S. Levit, Nucl. Phys. **A469**, 205 (1987).
[6] A. L. Goodman, Phys. Rev. C **33**, 2212 (1986); **34**, 1942 (1986).
[7] A. L. Goodman, Nucl. Phys. **A352**, 30 (1981).
[8] K. Tanabe, K. Sugawara-Tanabe, and H. J. Mang, Nucl. Phys. **A357**, 20 (1981).
[9] K. Kumar and M. Baranger, Nucl. Phys. **A110**, 529 (1968); **A110**, 490 (1968).
[10] S. T. Belyaev, Nucl. Phys. **24**, 322 (1961).
[11] I. Hamamoto, in *Nuclear Structure 1985,* edited by R. Broglia, G. B. Hagemann, and B. Herskind (Elsevier, Amsterdam, 1985), p. 129.
[12] A. Bohr and B. Mottelson, *Nuclear Structure* (Benjamin, Reading, 1975), Vol. II, p. 193.